

POZ/BTB and AT-hook-containing zinc finger protein 1 (PATZ1) inhibits endothelial cell senescence through a p53 dependent pathway

JH Cho¹, MJ Kim², KJ Kim³ and J-R Kim^{*1}

Vascular cell senescence, induced by the DNA damage response or inflammatory stress, contributes to age-associated vascular disease. Using complementary DNA microarray technology, we found that the level of POZ/BTB and AT-hook-containing zinc finger protein 1 (PATZ1) is downregulated during endothelial cell (EC) senescence. PATZ1 may have an important role as a transcriptional repressor in chromatin remodeling and transcription regulation; however, the role of PATZ1 in EC senescence and vascular aging remains unidentified. Knockdown of PATZ1 in young cells accelerated premature EC senescence, which was confirmed by growth arrest, increased p53 protein level and senescence-associated β -galactosidase (SA- β -gal) activity, and repression of EC tube formation. In contrast, overexpression of PATZ1 in senescent cells reversed senescent phenotypes. Cellular senescence induced by PATZ1 knockdown in young cells was rescued by knockdown of p53, but not by knockdown of p16^{INK4a}. PATZ1 knockdown increased ROS levels, and pretreatment with N-acetylcysteine abolished EC senescence induced by PATZ1 knockdown. Notably, PATZ1 immunoreactivity was lower in ECs of atherosclerotic tissues than those of normal arteries in LDLR^{-/-} mice, and immunoreactivity also decreased in ECs of old human arteries. These results suggest that PATZ1 may have an important role in the regulation of EC senescence through an ROS-mediated p53-dependent pathway and contribute to vascular diseases associated with aging.

Cell Death and Differentiation (2012) 19, 703–712; doi:10.1038/cdd.2011.142; published online 4 November 2011

Cellular senescence is an irreversible state of cell proliferation arrest, which can be caused by diverse factors, such as telomere shortening or dysfunction, oncogenic activation, chromatin perturbation, DNA damage, oxidative or inflammatory stresses, irradiation, cytotoxic drugs and so on.¹ Cellular senescence was first reported in normal human dermal fibroblasts after serial cultivation *in vitro*, designated as replicative senescence.² In addition to growth arrest, senescent cells show a variety of characteristic phenotypes including larger and flattened cell morphology,² increased activity of senescence-associated β -galactosidase (SA- β -gal),³ upregulation of p53 and p16^{INK4a} protein levels,⁴ DNA damage markers, such as γ H2AX and telomere dysfunction-induced foci,⁵ senescence-associated heterochromatic foci in the nucleus⁶ and secretion of inflammatory cytokines.⁷ A large body of evidence suggests that cellular senescence could be behind the process of organismal or tissue aging and may be an underlying mechanism for protection against cancer development due to uncontrolled proliferation.⁸ Organismal or tissue aging may be attributed to net accumulation of senescent cells in tissues and to limits on the regenerative

potential of stem cell pools.⁹ Oncogene activation during tumorigenesis induces cellular senescence, which limits cancer progression.⁴ Furthermore, cellular senescence may contribute to the pathophysiology of a variety of aging-associated diseases such as atherosclerosis, osteoarthritis, wound healing, benign prostate hyperplasia, etc.¹⁰ Regardless of heterogeneity in the underlying factors and biological markers associated with cellular senescence, accumulating evidence implicates the tumor suppressors, p53 and p16^{INK4a}/Rb, as the common major effectors of cellular senescence in normal somatic cells.⁸

PATZ1 (POZ/BTB and AT-hook-containing zinc finger protein 1), also named zinc finger protein 278 (ZNF278), MAZ-related factor (MAZR) and zinc finger sarcoma gene (ZSG), is a putative transcription regulator with 7 Cys2-His2-type zinc fingers.¹¹ PATZ1 is ubiquitously expressed in human tissues.¹² PATZ1 encodes 687 amino acids and is found at chromosome 22q12.¹³ Although the physiological role of PATZ1 is not clear, experimental evidence suggests that it is a potential transcription regulator.^{11,13,14} PATZ1 can function as a transcriptional repressor of basal transcription or

¹Department of Biochemistry and Molecular Biology, Aging-associated Vascular Disease Research Center, College of Medicine, Yeungnam University, Daegu, Republic of Korea; ²Department of Pathology, College of Medicine, Yeungnam University, Daegu, Republic of Korea and ³Department of Biomedical Laboratory Science, Tae Kyeung College, Gyeongsan, Republic of Korea

*Corresponding author: J-R Kim, Department of Biochemistry and Molecular Biology, Aging-associated Vascular Disease Research Center, College of Medicine, Yeungnam University, 317-1 Daemyung-Dong, Daegu 705-717, Republic of Korea. Tel: 82 53 620 4342; Fax: 82 53 654 6651. E-mail: kimjr@ynu.ac.kr

Keywords: cell aging; PATZ1; P53; ROS; vascular aging; atherosclerosis

Abbreviations: PATZ1, POZ/BTB and AT-hook-containing zinc finger protein 1; POZ, Poxvirus zinc finger; BTB, Bric-a-brac, Tramtrack, Broad-complex; SA- β -gal, senescence-associated β -galactosidase; HUVEC, human umbilical vascular endothelial cell; HDF, human dermal fibroblast; HDMEC, human dermal microvascular endothelial cell; RT-PCR, reverse transcription polymerase chain reaction; p53, tumor protein p53; ATM, Ataxia telangiectasia mutated; Rb, retinoblastoma protein; siRNA, small interfering RNA; shRNA, small hairpin RNA; NAC, N-acetylcysteine; MnSOD, manganese superoxide dismutase; ROS, reactive oxygen species; H2AX, H2A histone member X; LDLR, low density lipoprotein receptor.

Received 10.3.11; revised 12.9.11; accepted 27.9.11; Edited by JC Marine; published online 04.11.11

as a corepressor of RNF4 RING finger protein-mediated transcription activation on the c-myc, CDC6, galectin-1 and SV40 promoters.¹⁴ PATZ1 negatively regulates CD8 expression in double-negative thymocytes by binding to the CD8 enhancer and interacting with the nuclear receptor corepressor N-CoR complex.¹⁵ In contrast, PATZ1 acts as a transcriptional activator of the c-myc promoter in B cells, and transcriptional activation by BACH2 is enhanced by its interaction with the BTB/POZ domain of PATZ1.¹³

In carcinogenesis, PATZ1 has been found to fuse to the Ewing sarcoma gene (*EWS*) by a submicroscopic inversion of 22q, resulting in activation of *EWS* in soft tissue sarcoma, suggesting that PATZ1 might have a potential tumor suppressor function.¹⁶ PATZ1 could also be a potential proto-oncogene in colorectal cancer, as PATZ1 expression is increased in colorectal cancer tissues, PATZ1 upregulation promotes cell growth and its knockdown inhibits cell proliferation.¹² Recently, PATZ1 was reported to have a crucial role in normal male gametogenesis, and its upregulation and mislocalization from the nucleus to the cytosol was associated with the development of testicular tumors.¹⁷ Taken together, PATZ1 might be involved in the regulation of cell proliferation as a putative tumor suppressor or as an oncogene that regulates transcription, suggesting that PATZ1's role may still be somewhat controversial depending on cell context. Furthermore, as PATZ1 function in primary cells remains unclear, elucidation of PATZ1 function in the primary cell system may help shed light on its general functions.

The present study shows that the expression level of PATZ1 is decreased during cellular senescence of human umbilical vascular endothelial cells (HUVECs). Although knockdown of PATZ1 in young HUVECs accelerates cellular senescence, PATZ1 overexpression in old cells reverses senescence phenotypes. Furthermore, PATZ1-induced senescence is associated with ROS-mediated p53-dependent DNA damage responses. Notably, PATZ1 immunoreactivity decreases in endothelial cells (ECs) of atherosclerotic plaques in mice and of old arteries in humans. Our data suggest that PATZ1 has an important role in EC senescence through a p53-dependent signaling pathway and in vascular diseases associated with aging.

Results

Downregulation of PATZ1 in old HUVECs. PATZ1 was initially isolated to be repressed during cellular senescence in HUVECs by complementary DNA (cDNA) microarray technology (data not shown). Expression levels of PATZ1 mRNA and protein were further confirmed by RT-PCR and western blot analysis in young and old HUVECs. PATZ1 mRNA and protein levels were lower in old cells than in young cells (Figures 1a and b). In addition, a decrease in phosphorylated Rb and increases in p53, p21^{CIP1}, p16^{INK4a} and phosphorylated ATM were observed in old cells (Figure 1b). Shortening of telomere length was also confirmed in old cells (Figure 1c). As four alternatively spliced transcript variants and tissue/cell specific expression have been described for the *PATZ1* gene,¹⁸ we examined which variants was expressed in HUVECs. We found that

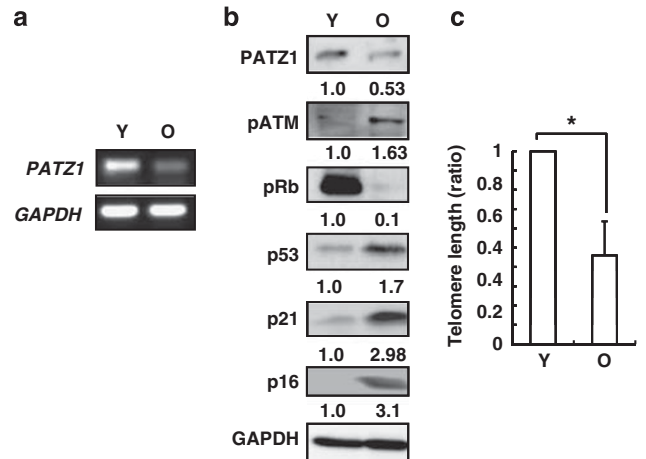


Figure 1 Downregulation of PATZ1 in old HUVECs. (a) RT-PCR analysis of PATZ1 levels in young (Y) and old (O) cells. Equal loading of RNA was estimated by GAPDH mRNA levels. (b) Western blotting for PATZ1, phospho-ATM (pATM), phospho-Rb (pRb), p53, p21^{CIP1} and p16^{INK4a} proteins. Equal loading of proteins was estimated by a GAPDH antibody. (c) Measurement of telomere length by realtime PCR. Representative data from three independent experiments are shown. Values are means \pm S.D. of three independent experiments. * $P < 0.05$ versus Y, young cells; O, old cells

variant 1 of PATZ1 (687 amino acids, about 74 kDa) was predominantly expressed in the protein levels in HUVECs, although four different transcripts of PATZ1 mRNA were observed in both cells by RT-PCR and dideoxy sequencing (Supplementary Figure 1).

Induction of cellular senescence by PATZ1 downregulation in young HUVECs. As the levels of PATZ1 mRNA and protein were decreased in old cells, we examined whether knockdown of PATZ1 accelerates cellular senescence. Young cells were transfected with PATZ1 siRNAs and downregulation of PATZ1 was confirmed by RT-PCR and western blotting (Figures 2a and f). In young HUVECs, PATZ1 knockdown caused cells to flatten, enlarge and become irregular in shape, with an increased diameter similar to old cells (Figure 2b). Knockdown of PATZ1 in young cells increased SA- β -gal staining activity (Figure 2b). Cell proliferation and bromodeoxyuridine (BrdU) incorporation were decreased in PATZ1 siRNA-transfected cells (Figures 2c and d). To confirm that PATZ1 siRNA cells entered senescence-related cell cycle arrest, cells were stained with propidium iodide, and DNA content was analyzed by flow cytometry. Although cell populations in S and G2/M phases were reduced, cells in G0/G1 increased in PATZ1 siRNA cells (Figure 2e), suggesting that PATZ1 knockdown induces G0/G1 cell cycle arrest, one of the typical phenotypes of cellular senescence.¹⁹

As pATM, p53, p21^{CIP1} and pRb protein levels are also known to be changed during cellular senescence,²⁰ we measured the levels of these proteins in PATZ1 siRNA cells. Expression levels of pATM, p53 and p21^{CIP1} proteins increased in PATZ1 siRNA cells (Figure 2f). Accumulation of phospho-H2AX foci was also enhanced in PATZ1 siRNA cells, suggesting that cellular senescence induced by PATZ1 knockdown is mediated through the ATM-dependent DNA damage signaling pathway (Figure 2g).

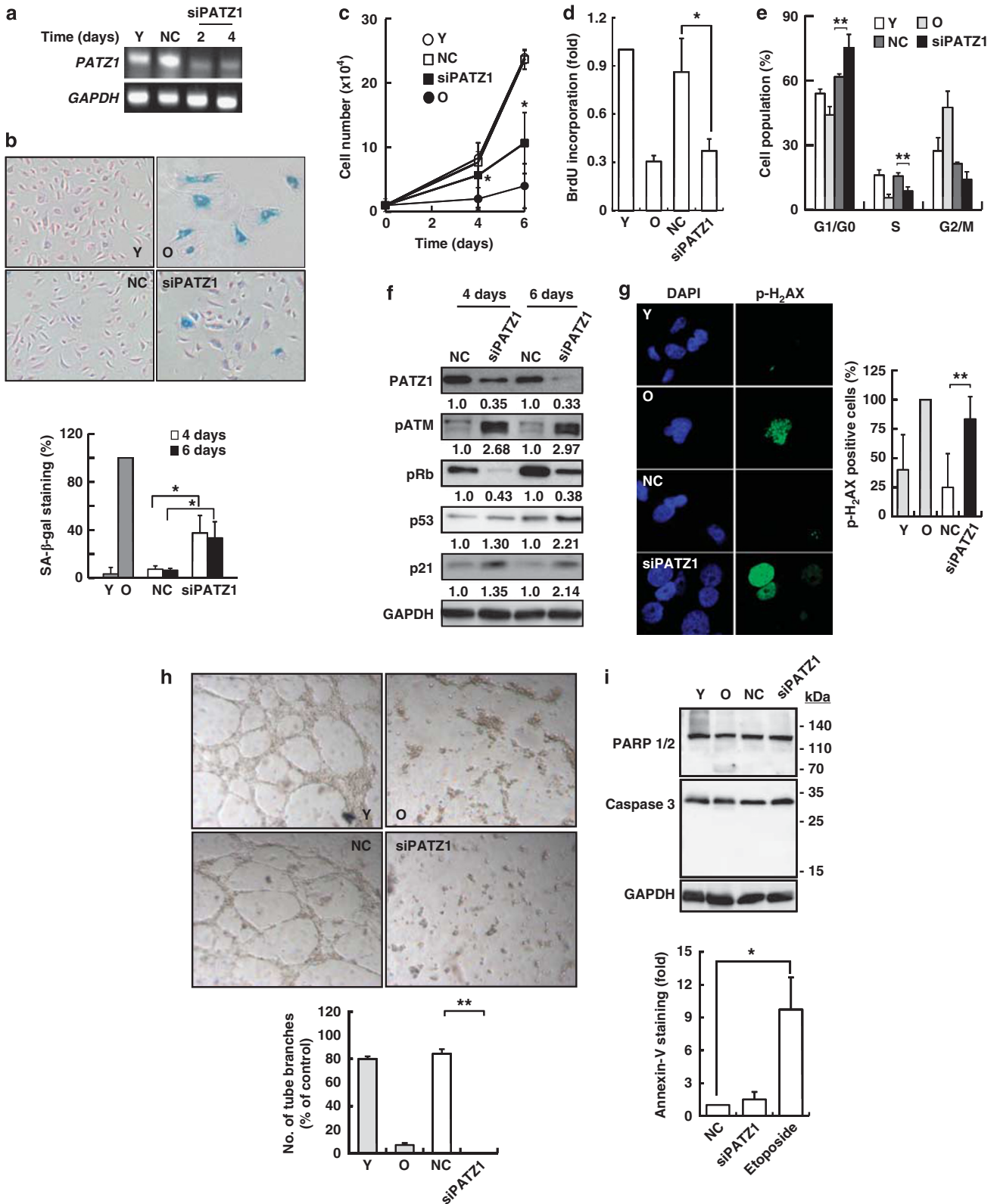


Figure 2 Induction of cellular senescence by PATZ1 knockdown. Young HUVECs were transfected with PATZ1 siRNA and incubated for the indicated times. (a) RT-PCR analysis of PATZ1 levels. Equal loading of RNA was estimated by the GAPDH mRNA levels. (b) SA- β -gal activity staining ($\times 100$) and the percentages of SA- β -gal positive cells in PATZ1 siRNA cells. (c) Cell proliferation measured by counting cells. * $P < 0.05$ versus control siRNA (NC). (d) BrdU incorporation analysis by flow cytometry. (e) Cell cycle profiles of PATZ1 siRNA cells. (f) Western blotting for PATZ1, pATM, pRb, p53 and p21^{CIP1} proteins in PATZ1 siRNA and control cells. (g) Accumulation of phospho-H₂AX in PATZ1 siRNA cells. (h) Tube formation in PATZ1 siRNA cells ($\times 40$). (i) Western blotting for PARP 1/2 and caspase 3 proteins and Annexin-V staining. Representative data from three independent experiments are shown. Values are means \pm S.D. of three independent experiments. * $P < 0.05$ or ** $P < 0.01$ versus NC, control siRNA; siPATZ1, PATZ1 siRNA

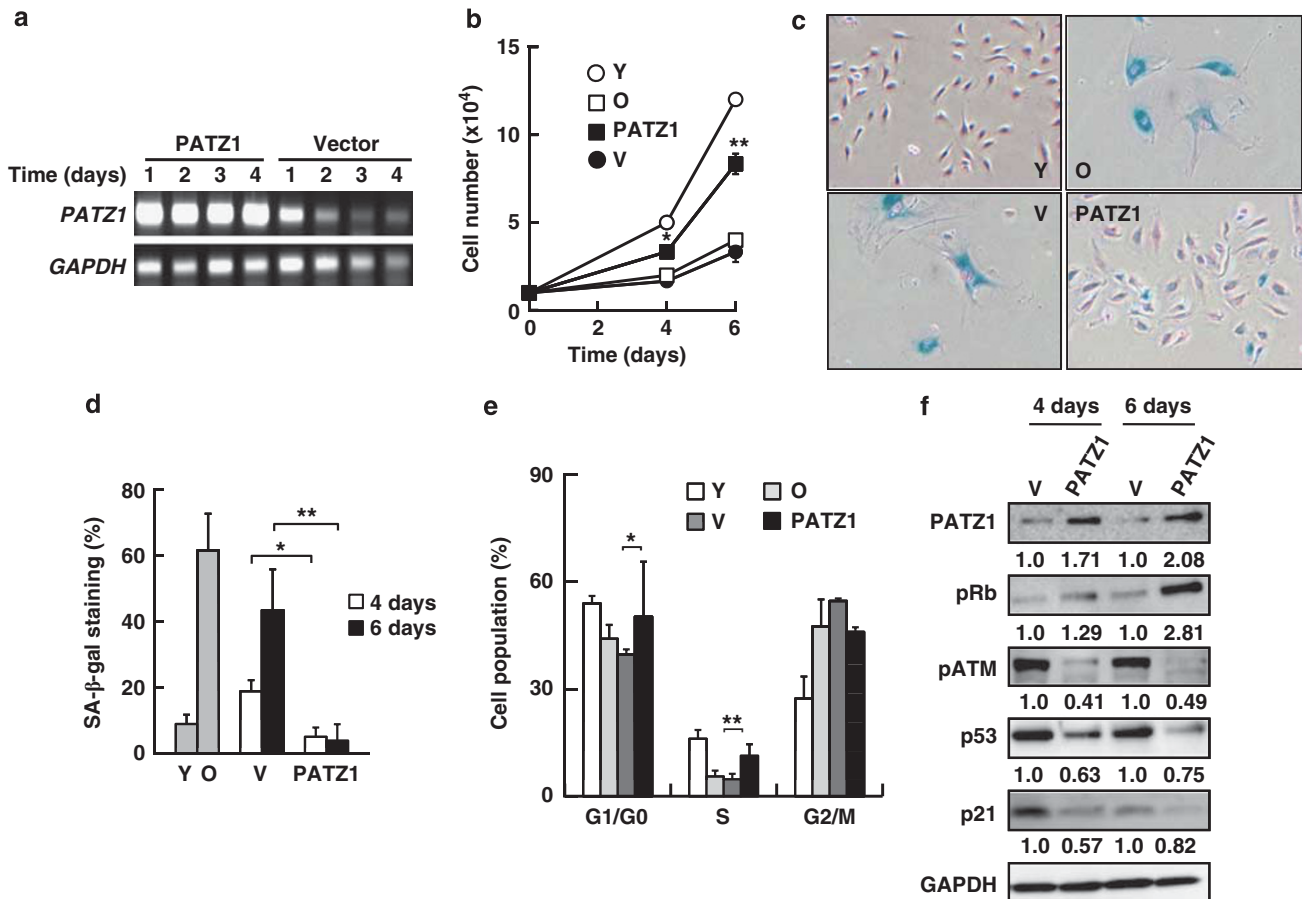


Figure 3 Reversal of cellular senescence by PATZ1 upregulation in old HUVECs. Old cells were transfected with pLenti6/V5/PATZ1 plasmids and incubated for 4 or 6 days. (a) RT-PCR analysis of PATZ1 mRNA levels. (b) Cell proliferation measured by counting cells. (c) SA- β -gal activity staining ($\times 100$). (d) Percentages of SA- β -gal positive cells. (e) Cell cycle profiles. (f) Western blotting for PATZ1, pATM, p53, pRb and p21^{CIP1} proteins. Representative data from three independent experiments are shown. Values are means \pm S.D. of three independent experiments. * $P < 0.05$ or ** $P < 0.01$ versus empty virus vector. V, pLenti6/V5 plasmids; PATZ1, pLenti6/V5/PATZ1 plasmids

HUVECs are known to form primitive blood vessels or tube structures *in vitro* following exposure to angiogenic factors.²¹ Although young HUVECs and control-siRNA transfected HUVECs grown in Matrigel showed tube formation, no tube formation was observed in old HUVECs and PATZ1-siRNA cells (Figure 2h). As PATZ1 was reported to induce apoptotic cell death in human glioma cells,²² we also measured the cleavages of caspase-3 and poly ADP ribose polymerase (PARP), and Annexin-V staining in PATZ1-siRNA cells. Cleavages of caspase-3 and PARP, and an increase in Annexin-V staining were not observed in PATZ1-knockdown cells (Figure 2i). This suggests that PATZ1 knockdown in HUVECs does not induce apoptosis, but rather accelerates cellular senescence in HUVECs.

In addition to HUVECs, we measured effects of PATZ1 knockdown in young human fibroblasts and human dermal microvascular endothelial cells. As expected, PATZ1 downregulation in young cells induced senescence phenotypes (Supplementary Figure 2 and Figure 3), suggesting that PATZ1 might have an important role in the regulation of cellular senescence in other primary cells.

Reversal of cellular senescence by PATZ1 overexpression in old HUVECs. As the PATZ1 level decreased in old cells, we examined whether overexpression of PATZ1 in old cells reverses the senescence phenotypes. Old cells were transfected with pLenti6/V5/PATZ1 plasmids, and upregulation of PATZ1 levels was confirmed by RT-PCR and western blotting (Figures 3a and f). Upregulation of PATZ1 in old cells increased cell proliferation (Figure 3b) and repressed SA- β -gal activity (Figures 3c and d). PATZ1 overexpression also released old cells from G2/M cell cycle arrest, confirmed by increases in G1/G0 and S-cell populations as visualized by flow cytometry (Figure 3e). In addition, PATZ1-overexpressing cells had decreased levels of phosphorylated-ATM, p53 and p21^{CIP1} proteins and increased phosphorylation of Rb at serine 807 and serine 811 (Figure 3f). PATZ1 upregulation also decreased SA- β -gal staining activity in old human fibroblasts (Supplementary Figure 4). These data suggest that PATZ1 upregulation in old cells reverses senescence phenotypes.

Induction of cellular senescence by PATZ1 knockdown through a p53-dependent pathway. The p53 and the

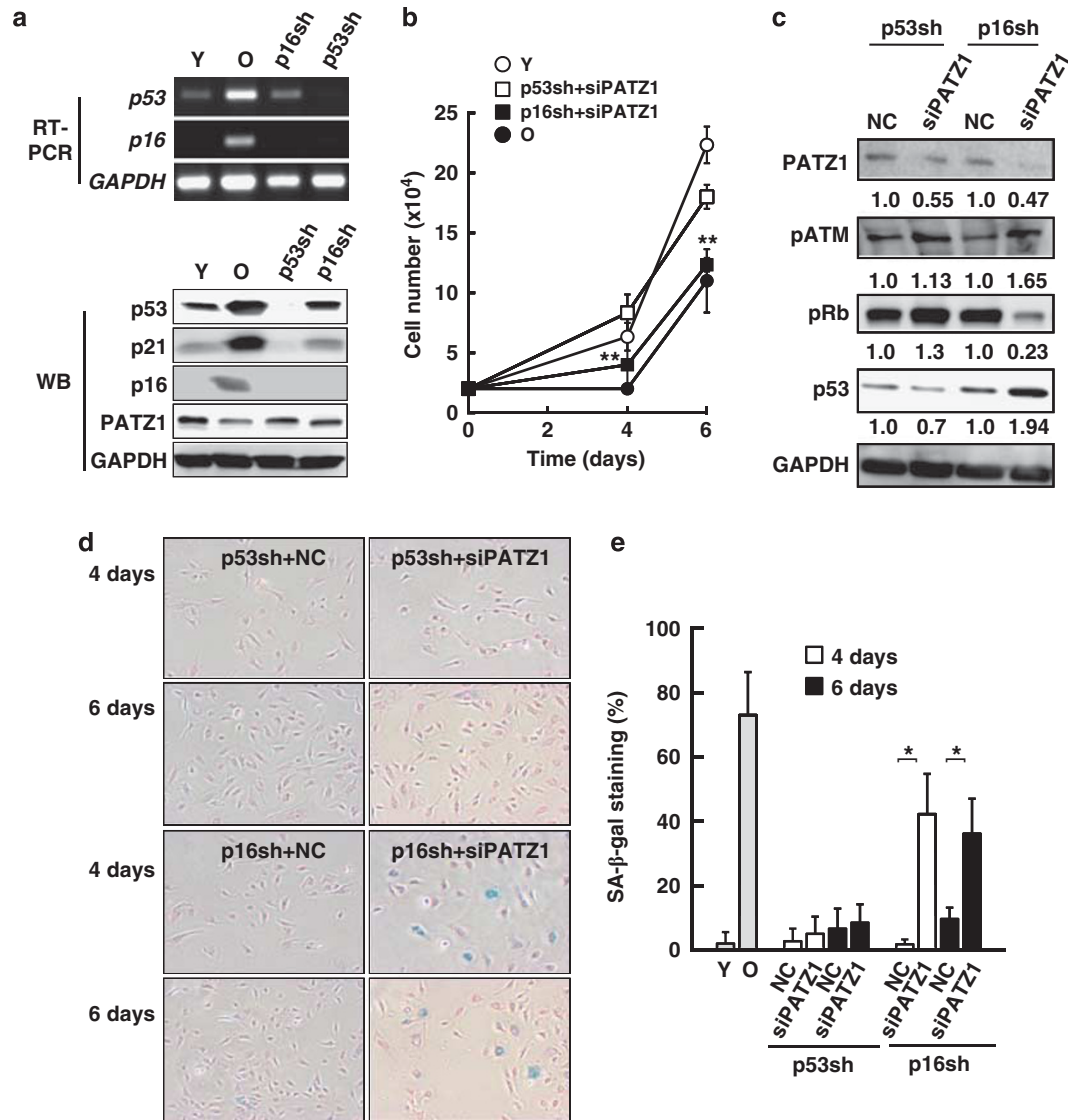


Figure 4 Induction of cellular senescence by PATZ1 knockdown through a p53-dependent pathway. Young HUVECs were transfected with p53 or p16^{INK4a} shRNA retroviral vectors and then transfected with PATZ1 siRNA. (a) RT-PCR analysis and western blotting to determine p53 and p16^{INK4a} levels. (b) Cell proliferation measured by counting cells. ***P* < 0.01 versus young cells. (c) Western blotting for PATZ1, pATM, pRb, and p53 proteins. (d) SA-β-gal activity staining (× 100). (e) Percentages of SA-β-gal-positive cells. Representative data from three independent experiments are shown. Values are means ± S.D. of three independent experiments. **P* < 0.05 or ***P* < 0.01 versus NC, control siRNA; p53sh, p53 shRNA retroviral vectors; p16sh, p16^{INK4a} shRNA retroviral vectors; siPATZ1, PATZ1 siRNA

p16^{INK4a}/Rb tumor suppressor pathways have a critical role in regulating cellular senescence in a variety of cells.⁸ Inactivation of these two pathways is well known to abolish cellular senescence.²³ To determine which pathway might be involved in cellular senescence by PATZ1 knockdown, we knocked down p53 or p16^{INK4a} levels using shRNA retroviral vectors in young HUVECs and measured the effects of PATZ1 on cellular senescence. Initially, knockdown of the levels of p53 or p16^{INK4a} mRNA and protein was confirmed by RT-PCR and western blotting (Figure 4a). Downregulation of p53 or p16^{INK4a} had no effect on the expression level of PATZ1 protein (Figure 4a) and SA-β-gal activity staining (Supplementary Figure 5). Downregulation of PATZ1 inhibited cell proliferation in p16^{INK4a}-knockdown cells, but not in p53-knockdown cells (Figure 4b). Although the level of

pRb protein decreased in the p16sh/PATZ1 siRNA cells, the p53 protein level increased compared with the other cells, particularly the p53sh/PATZ1 siRNA cells (Figure 4c). Transfection with PATZ1 siRNA increased SA-β-gal activity in p16^{INK4a}-knockdown cells, but not in p53-knockdown cells (Figures 4d and e). Therefore, these results suggest that PATZ1 knockdown-induced cellular senescence is mediated through a p53-dependent pathway.

Involvement of reactive oxygen species (ROS) in PATZ1-induced cellular senescence in HUVECs. To further investigate the mechanisms by which PATZ1 knockdown induces cellular senescence in HUVECs, we measured intracellular ROS levels in PATZ1 siRNA cells stained with Rhodamine 123. Fluorescent intensity of Rhodamine 123

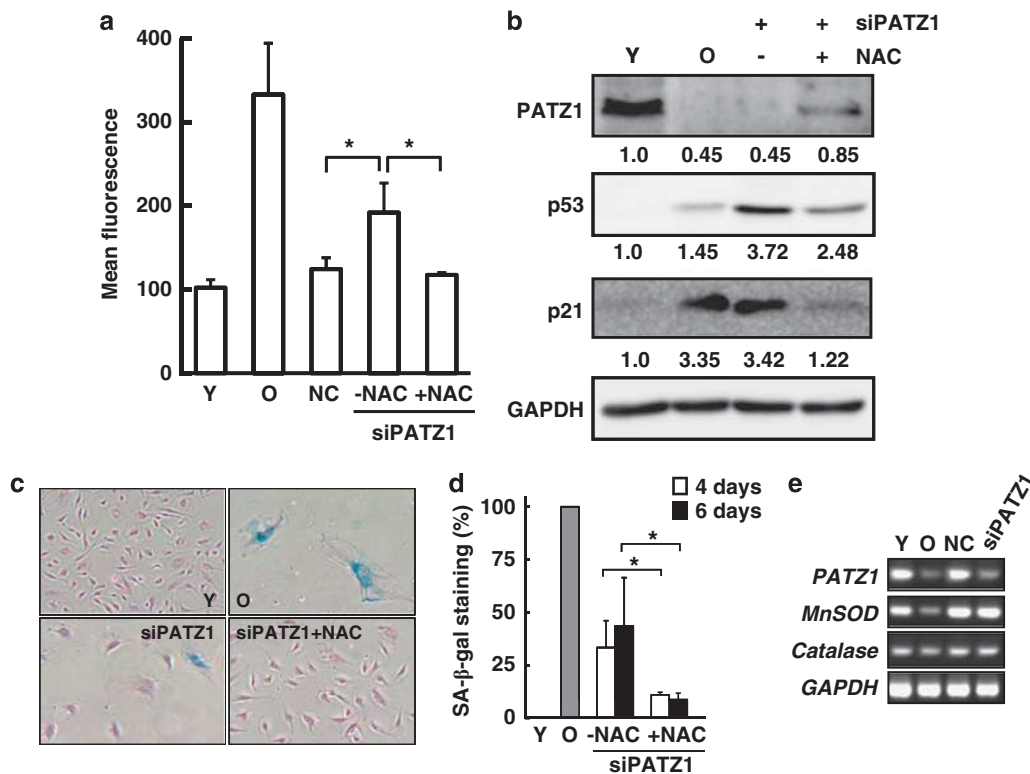


Figure 5 Involvement of reactive oxygen species in PATZ1-induced cellular senescence. Young HUVECs were transfected with PATZ1 siRNA for 4 days and treated with 10 $\mu\text{mol/l}$ dihydrorhodamine 123 for 30 min. (a) Flow cytometric analysis of rhodamine 123 fluorescence. PATZ1 siRNA cells were treated with or without 10 mM N-acetylcysteine for 4 days. (b) Western blotting for p53 and p21^{CIP1} proteins. (c) SA- β -gal activity staining ($\times 100$). (d) Percentages of SA- β -gal-positive cells. (e) RT-PCR for MnSOD and catalase. Representative data from three independent experiments are shown. Values are means \pm S.D. of three independent experiments. * $P < 0.05$ versus NC, control siRNA; NAC, N-acetylcysteine; siPATZ1, PATZ1 siRNA

was increased in PATZ1 siRNA cells (Figure 5a). Furthermore, pretreatment with N-acetylcysteine (NAC), a well-known antioxidant, reduced p53 and p21^{CIP1} protein levels that had been increased in PATZ1 siRNA cells (Figure 5b). Augmentation of SA- β -gal activity in PATZ1 siRNA cells was also decreased by NAC pretreatment (Figures 5c and d). We measured the levels of manganese superoxide dismutase (MnSOD) and catalase in PATZ1-siRNA cells whether PATZ1 knockdown increases ROS levels by regulating the expression levels of antioxidant enzymes in cells. PATZ1 knockdown had no effects on the expression levels of MnSOD and catalase mRNA (Figure 5e). These results imply that cellular senescence induced by PATZ1 knockdown is mediated through an ROS-dependent signal pathway.

Weak PATZ1 immunoreactivity in ECs of mouse atherosclerotic plaques and old human arteries. To investigate whether PATZ1 is involved in *in vivo* vascular aging and aging-associated vascular diseases, aortic sinus sections from LDLR^{-/-} mice with or without atherosclerotic lesions were stained for SA- β -gal activity and with a PATZ1 antibody. Blue cells showing SA- β -gal staining activity were observed only in atherosclerotic lesions of LDLR^{-/-} mice (Figure 6a). PATZ1 immunoreactivity was decreased in ECs and smooth muscle cells of atherosclerotic lesions compared

with normal aortic sinuses in LDLR^{-/-} mice (Figure 6b). PATZ1 immunoreactivity was also measured in arterial tissues obtained from young and old humans. As expected, immunopositive reactions to the PATZ1 antibody were weaker in ECs of old arteries than in those of young arteries (Figure 6c). These data suggest that PATZ1 might have an important role in vascular aging as well as in vascular diseases related to aging.

Discussion

The present study clearly shows the first evidence for the involvement of PATZ1 in cellular senescence of human primary ECs through the p53-dependent signal pathway. We also found that loss of PATZ1 expression is associated with vascular disease as well as vascular aging. We demonstrated that PATZ1 has an important role in cellular senescence of ECs through two different findings: (i) knock-down of PATZ1 in young cells induced cellular senescence, which was confirmed by growth arrest, an increase in p53 protein level and SA- β -gal activity, and the accumulation of phospho-H₂AX foci (Figure 2), and (ii) upregulation of PATZ1 in old cells reversed senescence phenotypes, such as a change in cell morphology, an increase in cell growth and a decrease in SA- β -gal activity (Figure 3).

PATZ1 contains an N-terminal POZ/BTB domain, an AT-hook domain and seven C2H2 zinc finger domains at the

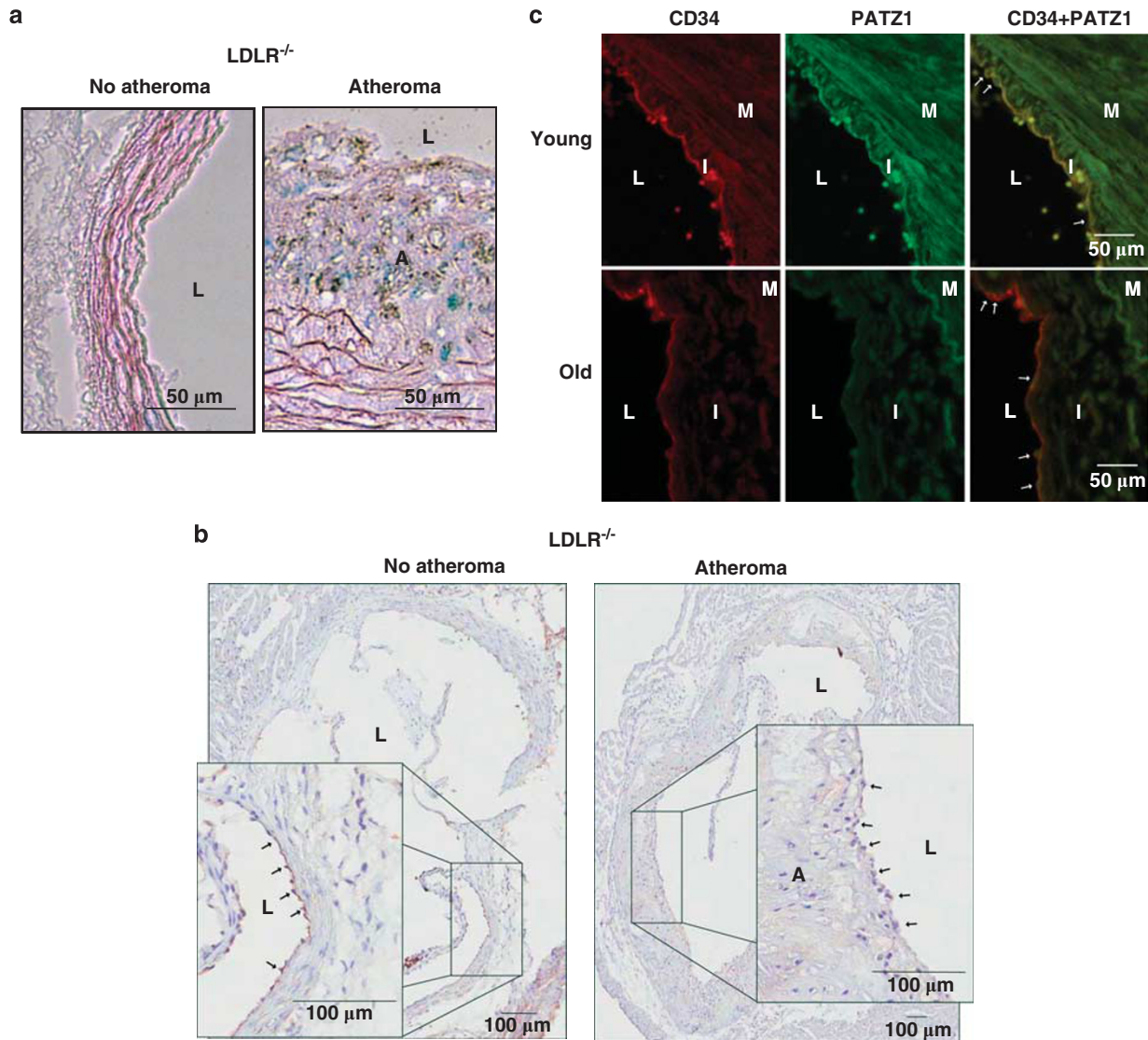


Figure 6 SA-β-gal activity staining and immunohistochemical staining of mouse atherosclerotic tissues or human arteries with a PATZ1 antibody. (a) SA-β-gal activity staining (blue) in aortic sinus sections of LDLR^{-/-} mice with or without atherosclerotic lesions. (b) PATZ1 immunoreactivity in aortic sinus sections of LDLR^{-/-} mice with or without atherosclerotic lesions. Insets show ×4 enlargement of the selected areas. (c) PATZ1 (green) and CD34 (red) immunoreactivity in young and old human arteries. Representative data from five independent specimens are shown. Arrows indicate ECs with the nucleus. L, lumen; A, atherosclerotic lesion; I, intima; M, media

C-terminus. The POZ (Poxvirus zinc finger) or BTB (Bric-a-brac, Tramtrack, Broad-complex) domain is widely distributed in many organisms and functions as a protein–protein interaction module. A variety of proteins, such as promyelocytic leukemia zinc finger (PLZF), BTB and CNC homolog 1 (BACH1), zinc finger and BTB-domain containing 2 and 5 (ZBTB2 and ZBTB5), and hypermethylated in cancer 1 (HIC1), are known to contain the POZ/BTB domain²⁴ and have been reported to regulate cell proliferation as well as cellular senescence. PLZF restricts proliferation of human cord blood-derived myeloid progenitor cells²⁵ and corneal ECs.²⁶ BACH1 inhibits p53-dependent premature cellular senescence in response to oxidative stress.²⁷ ZBTB2 was found to increase cell proliferation by repressing transcription of the *p21^{CIP1}* gene, a well known p53 target gene.²⁸ HIC1 suppresses age-dependent development of cancer by

mediating SIRT1- and p53-dependent apoptotic DNA damage responses.²⁹

One critical question has been determining what signal mediates the cellular senescence induced by PATZ1 knockdown in young HUVECs. Accumulating evidence suggests that p53/p21^{CIP1} and p16^{INK4a}/Rb tumor suppressor pathways are key regulators of the senescence response.⁸ We found that p53 is required for PATZ1 knockdown-induced cellular senescence: (i) PATZ1 knockdown decreased cell proliferation in p16-shRNA cells, but not in p53-shRNA cells (Figure 4b); (ii) PATZ1 knockdown decreased pRb protein levels and increased p53 protein levels in p16^{INK4a} knockdown cells (Figure 4c); (iii) PATZ1 knockdown induced increased SA-β-gal activity in p16-shRNA cells, but not in p53-shRNA cells (Figures 4d and e). The POZ/BTB proteins, such as HIC1, PLZF, BACH1, NAC-1 and BCL-6, have been

linked directly or indirectly to p53 regulation, and thereby linked to regulating cell proliferation.²⁴ ZBTB7A/FBI-1/Pokemon, one of the POK (POZ and Kruppel-like zinc finger) families, directly binds the p19Arf promoter and can repress its activity, resulting in oncogenic transformation through inhibition of p53 activity.³⁰ Furthermore, loss of ZBTB7A/Pokemon in mouse embryonic fibroblasts resulted in premature senescence and unresponsiveness to oncogenic stimuli, which was caused by aberrant upregulation of ARF.³¹ We showed that the level of phosphorylated-ATM was increased during premature cellular senescence induced by PATZ1 knockdown (Figure 2f) and was decreased in cells overexpressing PATZ1 (Figure 3f). As ATM activation has a critical role in p53-dependent DNA damage signaling,³² our results suggest that cellular senescence by PATZ1 knockdown might be mediated through ATM/p53-dependent DNA-damage responses.

ROS are known to trigger DNA-damage responses in p53-dependent cellular senescence.^{33,34} We found that ROS levels were increased in PATZ1-shRNA cells (Figure 5a), and pretreatment with N-acetylcysteine, a well known antioxidant, rescued senescence phenotypes induced by PATZ1 knockdown (Figures 5b–d), suggesting that PATZ1 knockdown may induce EC senescence through an ROS-mediated p53-dependent DNA damage response. In addition, some other proteins might also contribute to the regulation of cellular senescence induced by PATZ1 knockdown. One of POZ/BTB protein member, HIC1 was reported to bind to SIRT1 through its POZ domain.²⁹ As SIRT1 is known to modulate premature senescence-like phenotype in human ECs,³⁵ we measured binding of PATZ1 protein to SIRT1 by immunoprecipitation. We confirmed that the SIRT1 protein level decreased in old cells and PATZ1 was bound to SIRT1 (Supplementary Figure 6). Further studies on the regulation of SIRT1 by PATZ1 would be necessary to elucidate the role of PATZ1 in the regulation of cellular senescence.

Cellular senescence has been thought to contribute to *in vivo* tissue aging and aging-associated diseases, such as atherosclerosis.³⁶ Atherosclerosis is a complex, chronic and inflammatory disease of the vasculature with lesions developing in the arterial wall.³⁷ An activated DNA damage response pathway induced by both oxidative stress and telomere dysfunction may be a crucial mediator for vascular senescence via activation of the p53/p21^{CIP1} and p16^{INK4a}/Rb pathways, which in turn contribute to the pathogenesis of atherosclerosis.³⁸ Our results suggest that PATZ1 may induce these pathways in ECs, and thus contribute to vascular aging and the development of aging-associated cardiovascular diseases.

Materials and Methods

Materials. Human umbilical vein endothelial cells (HUVECs) and endothelial cell basal medium-2 (EBM-2) containing several growth factors and supplements (EGM-2) were from LONZA Inc., (Walkersville, MD, USA). The primers used for polymerase chain reaction of PATZ1 (forward, 5'-ACTTGGGCTCCCTTTGG-3'; reverse, 5'-GC ACTGGATGCCACTG-3'; 229 bp), MnSOD (forward, 5'-TTGGCCAAGGGAGAT GTTAC-3'; reverse, 5'-CTGATTTGGACAAGCAGCAA-3'), catalase (forward, 5'-AG GCCAGTCCTGACAAAATG-3'; reverse, 5'-GAATCTCCGCATTCTCCAG-3'), and GAPDH (forward, 5'-CGACCACCTTTGTCAAGCTCA-3'; reverse, 5'-AGGGGTCTA CATGGCAACTG-3'), and the primers to clone full-length cDNA of PATZ1 (GenBank Accession Number, BC021091) (forward, 5'-CACCATGGAGCGGGTGAACG-3';

reverse, 5'-GCCAACAGGCCACTGGTAAA-3') were synthesized from Bioneer Inc., (Daejeon, Republic of Korea). Antibodies against PATZ1 (P-17, sc-86778), PARP-1/2, caspase-3 and p53, FITC-conjugated goat anti-rabbit IgG and TR-conjugated goat anti-mouse IgG were obtained from Santa Cruz Biotech Inc., (Santa Cruz, CA, USA). Antibodies against p21^{CIP1}, phospho-ATM and phospho-Rb were purchased from Cell Signaling Technology Inc., (Beverly, MA, USA). A CD34 antibody was from Cell Marque Corp., (Rocklin, CA, USA). A Polink-2 HRP plus rabbit DAB detection system was from Golden Bridge International, Inc., (Mukilteo, WA, USA). A rabbit polyclonal anti-glyceraldehyde 3-phosphate dehydrogenase (GAPDH) was kindly provided by Dr. K S Kwon (KRIBB, Daejeon, Republic of Korea). The pLenti6/V5 directional TOPO cloning kit was from Invitrogen Inc. (Carlsbad, CA, USA). The full-sequence PATZ1 gene was from Open Biosystems Inc., (Huntsville, AL, USA). Stealth siRNAs for PATZ1 (sense, 5'-AACCGACCUCAUCAGCAGGAACUUG-3' and antisense, 5'-CAAGUCCU GCUGAUGAGGUCGGUU-3') and control siRNA (sense, 5'-UUCUCCGACGUGUC ACGU-3' and antisense, 5'-ACGUGACACGUUCGAGAA-3') were from Invitrogen Life Technologies. The pRetroSuper-p53sh and pRetroSuper-p16sh vectors were provided by Dr. R Agami (Division of Tumor Biology, The Netherlands Cancer Institute, Amsterdam, The Netherlands). A total of five aortic sinus sections with or without atherosclerotic lesions from LDLR^{-/-} mice were kindly donated by G T Oh (Ewha Womans University, Seoul, Republic of Korea). Vascular specimens from young and old patients were obtained from the Department of Pathology of Yeungnam University Hospital (Daegu, Republic of Korea) from 2000 to 2007: young normal patients ($n = 5$; average, 16 years old) and old normal patients ($n = 5$; average, 64 years old).

Cell culture. HUVECs in EGM-2 media were cultured as previously described.³⁹ For the experiments, cells were used at either passage 7 (PD < 28) or passage 15 (PD > 50). These are referred to as 'young' and 'old' cells, respectively.

Total RNA extraction, reverse transcription-polymerase chain reaction (RT-PCR). Total RNA was isolated from cells using the Trizol reagent (Invitrogen Life Technologies Inc.) according to the manufacturer's instructions. cDNA was synthesized from total RNA using MMLV reverse transcriptase (Promega Corp., Madison, WI, USA) and target DNA sequences were amplified by PCR.³⁹ GAPDH primers were used to standardize the amount of RNA in each sample.

Protein extraction. Cells were washed with ice-cold phosphate-buffered saline (PBS) and lysed in 100 μ l of ice-cold RIPA buffer. After centrifugation, protein concentrations in the supernatants were quantified by the bicinchoninic acid (BCA) method (Pierce Biotechnology Inc., Rockford, IL, USA) using bovine serum albumin as a standard.

Western blot analysis. Proteins were separated on 12 or 10% SDS-polyacrylamide gels and then transferred to nitrocellulose membranes. Primary antibodies against pATM, pRb, PATZ1, p53 and p21^{CIP1} were applied overnight at 4 °C, and then HRP-conjugated, goat anti-mouse or anti-rabbit (1 : 3000) antibodies were applied. Antigen-antibody complexes were detected using western blotting Luminol Reagent (Santa Cruz Biotech Inc.). Images of membranes were captured using a LAS-3000 image system (Fujifilm Inc., Stamford, CT, USA). The relative intensities of protein bands, as compared with that of the respective GAPDH signal, were determined by using the Multi Gauge software, version 3.0 (Fujifilm Inc.), and normalized to 1.0 for control cells by averaging three separate experiments.

Measurement of telomere length by realtime PCR. Telomere length was measured by telomeric repeat amplification using realtime PCR.⁴⁰ Genomic DNAs were extracted using Chelex 100 Resin (Bio-Rad Laboratories Inc., Hercules, CA, USA). Telomere length in each of genomic DNA was analyzed with telomere primers (tel 1, 5'-GGTTTTGAGGGTGAGGGTGAGGGTGAGGGTGAGGGT-3'; tel 2, 5'-TCCCGACTATCCCTATCCCTATCCCTATCCCTATCCCTA-3') and with 36B4 single-copy telomere gene primers (36B4u, 5'-CAGCAAGTGGGAAGGTG TAATCC-3'; 36B4d, 5'-CCCATTCTATCATCAACGGGTACAA-3'). Real-time PCR was conducted using SYBR Green PCR master mix (Applied Biosystems Inc., Carlsbad, CA, USA) and the LightCycler 2.0 Real-Time PCR system (Roche Diagnostic Corp., Indianapolis, IN, USA).

Preparation and transfection of pLenti6/V5/PATZ1 plasmids. For overexpression of PATZ1, the pLenti6/V5/PATZ1 plasmid was prepared according to the manufacturer's instructions (Invitrogen Life Technologies Inc.). PATZ1 cDNA was amplified from the pOTB7/PATZ1 plasmids by PCR and cloned into a pLenti6/V5-D-TOPO vector. Nucleotide sequences of PATZ1 were confirmed by dideoxy

sequencing. Old HUVECs (4×10^5) were seeded in 100 mm dishes and incubated 24 h in EGM-2 media. Cells were then transfected with the pLenti6/V5/PATZ1 plasmids or empty vector as a control using the FuGene HD Transfection Reagent (Roche Ltd, Basel, Switzerland) according to the manufacturer's protocol. After overnight incubation, fresh growth media were exchanged, and the PATZ1 protein level was measured by western blotting with a PATZ1 antibody.

Transfection of PATZ1 siRNA. For knockdown of PATZ1, Stealth siRNAs specific for PATZ1 (160 nmol/l) were transfected into young HUVECs using the Lipofectamine 2000 transfection reagent (Life Technologies Inc., Gaithersburg, MD, USA) according to the manufacturer's directions. Knockdown of PATZ1 RNA and protein levels was measured by RT-PCR and western blotting with a PATZ1 antibody, respectively.

Cell staining. The proportion of senescent HUVECs or senescent cells in atherosclerotic tissues of LDLR^{-/-} mice was determined by measuring senescence associated- β -galactosidase (SA- β -gal) activity as described previously.³ Rhodamin-conjugated phalloidin and 4',6-diamidino-2-phenylindole (DAPI) staining was performed. For measuring the levels of phospho-H2AX protein, cells were washed with ice-cold PBS, fixed with 3.7% (v/v) paraformaldehyde in PBS for 10 min, and permeabilized with 0.5% Triton X-100 in PBS for 5 min. A phospho-H2AX (ser139) antibody conjugated with Alexa Fluor 488 (BioLegend, San Diego, CA, USA) was applied for 2.5 h and the nuclei were stained with DAPI. Cells were observed with a fluorescence microscope.

Cell cycle analysis by flow cytometry. The cell cycle profiles were measured by staining with propidium iodide.³⁹ The intracellular propidium iodide fluorescence intensity of each population of 10 000 cells was measured in each sample using a Becton–Dickinson FACS Canto II flow cytometer (BD Bioscience, San Jose, CA, USA).

Annexin-V staining. Cells were incubated with 10 mM HEPES, 140 mM NaCl, 2.5 mM CaCl₂, pH 7.4 containing Alexa Fluor 647-conjugated Annexin-V (Invitrogen) and Annexin-V binding was analyzed using the Becton–Dickinson FACS Canto II flow cytometer (BD Bioscience).

Measurement of BrdU incorporation. Cells were transfected with PATZ1 siRNA or control siRNA and incubated for 2 days. Intracellular BrdU incorporation was measured using the BrdU flow kit (BD Bioscience) according to the manufacturer's protocol and analyzed using a Becton–Dickinson FACS Canto II flow cytometer (BD Bioscience).

Transfection of p53 or p16^{INK4a} shRNA retroviral vectors in young HUVECs. To knockdown p53 and p16^{INK4a}, transient transfection of young HUVECs with the pRetroSuper-p16sh or the pRetroSuper-p53sh vector was carried out using the FuGene HD Transfection Reagent (Roche Ltd) according to the manufacturer's protocol. p16 shRNA or p53 shRNA-knockdown cells were transfected further with PATZ1 Stealth siRNAs using the Lipofectamine 2000 transfection reagent (Life Technologies Inc.) according to the manufacturer's protocol. After incubation for 4 days, knockdown of p16^{INK4a} or p53 RNA levels was confirmed by RT-PCR, and SA- β -gal activity in transfected cells was measured.

Intracellular ROS measurement with dihydrorhodamine 123. ROS production was determined by using dihydrorhodamine123 as a fluorescence probe. Intracellular Rhodamine 123 fluorescence intensity was measured using a Becton–Dickinson FACS Canto II flow cytometer (BD Bioscience).

EC tube formation assay. In all 96-well plates were coated with 65 μ l of Matrigel (BD Bioscience). Young HUVECs (2.5×10^4 cells/well) transfected with PATZ1 or control siRNAs were plated in duplicate and incubated at 37 °C for 4 h. Tube formation was observed with a light microscope.

Immunohistochemical staining. Formalin-fixed and paraffin-embedded tissues were immunohistochemically stained to detect PATZ1 levels. Aortic sinus sections of LDLR^{-/-} mice were stained with a rabbit polyclonal PATZ1 antibody (dilution 1 : 50) and visualized by the Polink-2 HRP plus rabbit DAB detection system (Golden Bridge International, Inc.). Human vascular tissue samples were double stained with a rabbit polyclonal PATZ1 antibody (dilution 1 : 20) and a mouse

monoclonal CD34 antibody (dilution 1 : 50). FITC-conjugated goat anti-rabbit IgG (dilution 1 : 100) and TR-conjugated goat anti-mouse IgG (dilution 1 : 100) were applied as secondary antibodies. As a negative control, the primary antibody was replaced with non-immune serum. Photographs were taken with a Leica DM6000B fluorescence microscope (Leica Microsystems GmbH, Wetzlar, Germany).

Statistical analysis. All values are presented as means \pm S.D. The Student's *t*-test was employed for all analyses. A *P*-value < 0.05 was considered statistically significant.

Conflict of Interest

The authors declare no conflict of interest.

Acknowledgements. This work was supported by the National Research Foundation of Korea (NRF) grant funded by the Korea government (MEST) (2011-0001241).

- Collado M, Serrano M. The power and the promise of oncogene-induced senescence markers. *Nat Rev Cancer* 2006; **6**: 472–476.
- Hayflick L, Moorhead PS. The serial cultivation of human diploid cell strains. *Exp Cell Res* 1961; **25**: 585–621.
- Dimri GP, Lee X, Basile G, Acosta M, Scott G, Roskelley C *et al*. A biomarker that identifies senescent human cells in culture and in aging skin *in vivo*. *Proc Natl Acad Sci USA* 1995; **92**: 9363–9367.
- Serrano M, Lin AW, McCurrach ME, Beach D, Lowe SW. Oncogenic ras provokes premature cell senescence associated with accumulation of p53 and p16INK4a. *Cell* 1997; **88**: 593–602.
- Fumagalli M, d'Adda di Fagagna F. SASPense and DDRama in cancer and ageing. *Nat Cell Biol* 2009; **11**: 921–923.
- Narita M, Nunez S, Heard E, Narita M, Lin AW, Hearn SA *et al*. Rb-mediated heterochromatin formation and silencing of E2F target genes during cellular senescence. *Cell* 2003; **113**: 703–716.
- Kuilman T, Peeper DS. Senescence-messaging secretome: SMS-ing cellular stress. *Nat Rev Cancer* 2009; **9**: 81–94.
- Campisi J, d'Adda di Fagagna F. Cellular senescence: when bad things happen to good cells. *Nat Rev Mol Cell Biol* 2007; **8**: 729–740.
- Collado M, Blasco MA, Serrano M. Cellular senescence in cancer and aging. *Cell* 2007; **130**: 223–233.
- Jeyapalan JC, Sedivy JM. Cellular senescence and organismal aging. *Mech Ageing Dev* 2008; **129**: 467–474.
- Pero R, Lembo F, Palmieri EA, Vitiello C, Fedele M, Fusco A *et al*. PATZ attenuates the RNF4-mediated enhancement of androgen receptor-dependent transcription. *J Biol Chem* 2002; **277**: 3280–3285.
- Tian X, Sun D, Zhang Y, Zhao S, Xiong H, Fang J. Zinc finger protein 278, a potential oncogene in human colorectal cancer. *Acta Biochim Biophys Sin (Shanghai)* 2008; **40**: 289–296.
- Kobayashi A, Yamagiwa H, Hoshino H, Muto A, Sato K, Morita M *et al*. A combinatorial code for gene expression generated by transcription factor Bach2 and MAZR (MAZ-related factor) through the BTB/POZ domain. *Mol Cell Biol* 2000; **20**: 1733–1746.
- Fedele M, Benvenuto G, Pero R, Majello B, Battista S, Lembo F *et al*. A novel member of the BTB/POZ family, PATZ, associates with the RNF4 RING finger protein and acts as a transcriptional repressor. *J Biol Chem* 2000; **275**: 7894–7901.
- Bilic I, Koesters C, Unger B, Sekimata M, Hertweck A, Maschek R *et al*. Negative regulation of CD8 expression via Cd8 enhancer-mediated recruitment of the zinc finger protein MAZR. *Nat Immunol* 2006; **7**: 392–400.
- Mastrangelo T, Modena P, Tornielli S, Bullrich F, Testi MA, Mezzelani A *et al*. A novel zinc finger gene is fused to EWS in small round cell tumor. *Oncogene* 2000; **19**: 3799–3804.
- Fedele M, Franco R, Salvatore G, Paronetto MP, Barbagallo F, Pero R *et al*. PATZ1 gene has a critical role in the spermatogenesis and testicular tumours. *J Pathol* 2008; **215**: 39–47.
- Esposito F, Boscia F, Franco R, Tornincasa M, Fusco A, Kitazawa S *et al*. Down-regulation of oestrogen receptor-beta associates with transcriptional co-regulator PATZ1 delocalization in human testicular seminomas. *J Pathol* 2011; **224**: 110–120.
- Wagner M, Hampel B, Bernhard D, Hala M, Zwerschke W, Jansen-Durr P. Replicative senescence of human endothelial cells *in vitro* involves G1 arrest, polyploidization and senescence-associated apoptosis. *Exp Gerontol* 2001; **36**: 1327–1347.
- Atadja P, Wong H, Garkavtsev I, Veillette C, Riabowol K. Increased activity of p53 in senescing fibroblasts. *Proc Natl Acad Sci USA* 1995; **92**: 8348–8352.
- Akhtar N, Dickerson EB, Auerbach R. The sponge/Matrigel angiogenesis assay. *Angiogenesis* 2002; **5**: 75–80.

22. Tritz R, Mueller BM, Hickey MJ, Lin AH, Gomez GG, Hadwiger P *et al*. siRNA Down-regulation of the PATZ1 Gene in Human Glioma Cells Increases Their Sensitivity to Apoptotic Stimuli. *Cancer Ther* 2008; **6**: 865–876.
23. Ye X, Zerlanko B, Zhang R, Somaiah N, Lipinski M, Salomoni P *et al*. Definition of pRB- and p53-dependent and -independent steps in HIRA/ASF1a-mediated formation of senescence-associated heterochromatin foci. *Mol Cell Biol* 2007; **27**: 2452–2465.
24. Kelly KF, Daniel JM. POZ for effect—POZ-ZF transcription factors in cancer and development. *Trends Cell Biol* 2006; **16**: 578–587.
25. Doulatov S, Notta F, Rice KL, Howell L, Zelent A, Licht JD *et al*. PLZF is a regulator of homeostatic and cytokine-induced myeloid development. *Genes Dev* 2009; **23**: 2076–2087.
26. Joko T, Nanba D, Shiba F, Miyata K, Shiraishi A, Ohashi Y *et al*. Effects of promyelocytic leukemia zinc finger protein on the proliferation of cultured human corneal endothelial cells. *Mol Vis* 2007; **13**: 649–658.
27. Dohi Y, Ikura T, Hoshikawa Y, Katoh Y, Ota K, Nakanome A *et al*. Bach1 inhibits oxidative stress-induced cellular senescence by impeding p53 function on chromatin. *Nat Struct Mol Biol* 2008; **15**: 1246–1254.
28. Jeon BN, Choi WI, Yu MY, Yoon AR, Kim MH, Yun CO *et al*. ZBTB2, a novel master regulator of the p53 pathway. *J Biol Chem* 2009; **284**: 17935–17946.
29. Chen WY, Wang DH, Yen RC, Luo J, Gu W, Baylin SB. Tumor suppressor HIC1 directly regulates SIRT1 to modulate p53-dependent DNA-damage responses. *Cell* 2005; **123**: 437–448.
30. Maeda T, Hobbs RM, Merghoub T, Guernah I, Zelent A, Cordon-Cardo C *et al*. Role of the proto-oncogene Pokemon in cellular transformation and ARF repression. *Nature* 2005; **433**: 278–285.
31. Maeda T, Hobbs RM, Pandolfi PP. The transcription factor Pokemon: a new key player in cancer pathogenesis. *Cancer Res* 2005; **65**: 8575–8578.
32. Bartek J, Bartkova J, Lukas J. DNA damage signalling guards against activated oncogenes and tumour progression. *Oncogene* 2007; **26**: 7773–7779.
33. Moiseeva O, Mallette FA, Mukhopadhyay UK, Moores A, Ferbeyre G. DNA damage signaling and p53-dependent senescence after prolonged beta-interferon stimulation. *Mol Biol Cell* 2006; **17**: 1583–1592.
34. Kim KS, Kang KW, Seu YB, Baek SH, Kim JR. Interferon-gamma induces cellular senescence through p53-dependent DNA damage signaling in human endothelial cells. *Mech Ageing Dev* 2009; **130**: 179–188.
35. Ota H, Akishita M, Eto M, Iijima K, Kaneki M, Ouchi Y. Sirt1 modulates premature senescence-like phenotype in human endothelial cells. *J Mol Cell Cardiol* 2007; **43**: 571–579.
36. Minamino T, Komuro I. Vascular cell senescence: contribution to atherosclerosis. *Circ Res* 2007; **100**: 15–26.
37. Ross R. Atherosclerosis—an inflammatory disease. *New Eng J Med* 1999; **340**: 115–126.
38. Andreassi MG. DNA damage, vascular senescence and atherosclerosis. *J Mol Med (Berlin, Germany)* 2008; **86**: 1033–1043.
39. Kim KS, Kim MS, Seu YB, Chung HY, Kim JH, Kim JR. Regulation of replicative senescence by insulin-like growth factor-binding protein 3 in human umbilical vein endothelial cells. *Aging cell* 2007; **6**: 535–545.
40. Cawthon RM. Telomere measurement by quantitative PCR. *Nucleic Acids Res* 2002; **30**: e47.

Supplementary Information accompanies the paper on Cell Death and Differentiation website (<http://www.nature.com/cdd>)